Electronic Supplementary Material (ESI) for Journal of Materials Chemistry C.

Electronic Supporting Information

Electric Field Tailored Giant Transformation of Magnetic Anisotropy and Interfacial Spin Coupling in Epitaxial γ'-Fe_4N/$Pb(Mg_{1/3}Nb_{2/3})_{0.7}Ti_{0.3}O_3$(011) Multiferroic Heterostructures

Zhengxun Lai,[a] Chunlei Li,[b] Zirun Li,[a] Xiang Liu,[a] Ziyao Zhou,[b] Wenbo Mi,[*a] Ming Liu[*b]

[a]*Tianjin Key Laboratory of Low Dimensional Materials Physics and Preparation Technology, School of Science, Tianjin University, Tianjin 300354, China*

[b]*Electronic Materials Research Laboratory, Key Laboratory of the Ministry of Education & International Center for Dielectric Research, Xi'an Jiaotong University, Xi'an 710049, China*

[*]Author to whom all correspondence should be addressed.

E-mail: miwenbo@tju.edu.cn
E-mail: mingliu@xjtu.edu.cn

1. Piezoelectric force microscopy (PFM) phase images of the PMN-PT(011) substrate

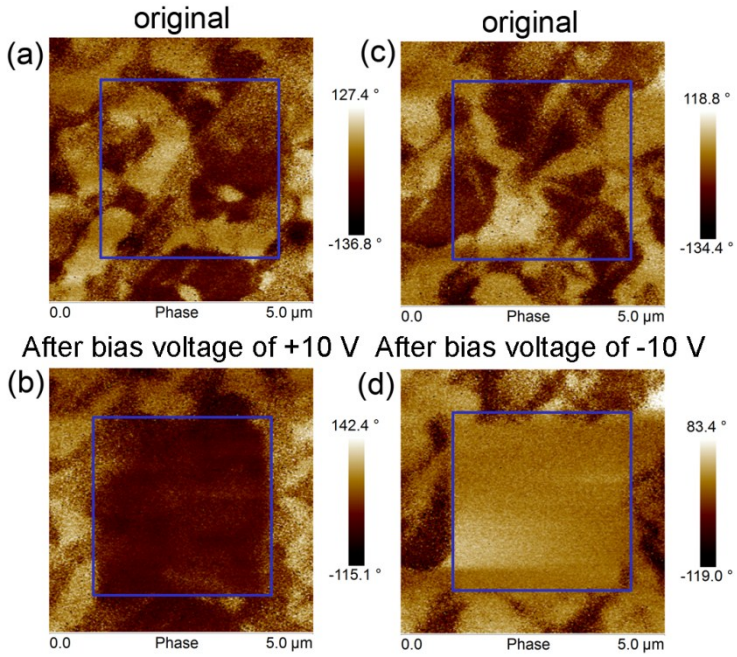

FIG. S1. (a) and (c) are the original out-of plane piezoelectric force microscopy (PFM) images of PMN-0.3PT(011) in a 5×5 μm^2 area, (b) and (d) are the images of the same area after applying a probe bias switching (+10 or -10 V) in a 3×3 μm^2 area.

Figs. S1(a)-(d) show PFM phase images of the PMN-PT(011) substrate. Fig. S1(a) and (c) are the original PFM phase images without polarization, (b) and (d) are the images after a probe bias switching (+10 or -10 V) applied in a 3×3 μm^2 area of the PMN-PT substrates. One can see the out-of-plane polarization states point to the same direction sharply after polarization, which indicates a perfect ferroelectricity.

2. Electric field control on the *M-H* curves of γ'-Fe_4N/PMN-PT(011) heterostructure with a 60-nm-thick γ'-Fe_4N film

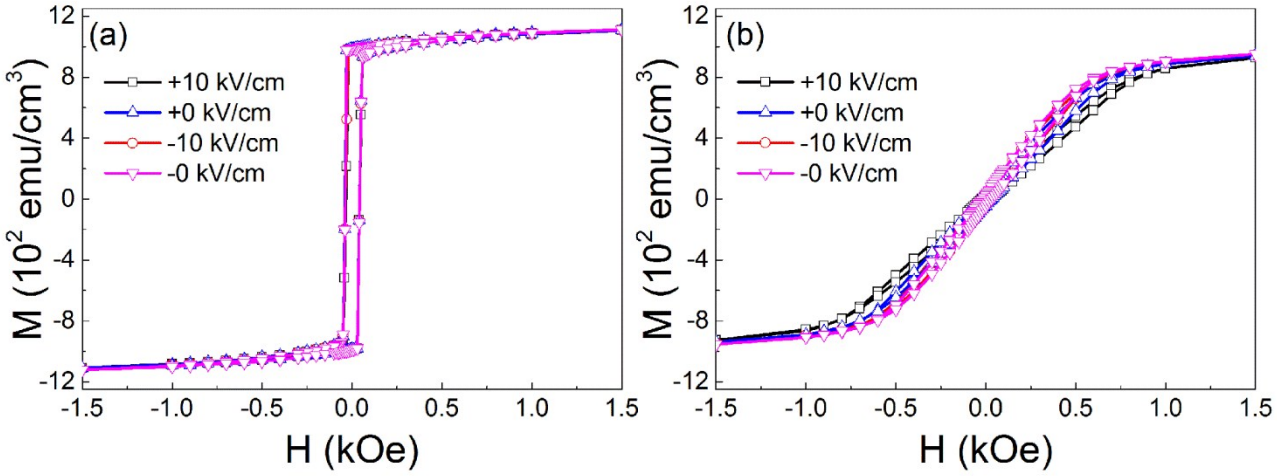

FIG. S2. The *M-H* curves of the γ'-Fe_4N/PMN-PT(011) heterostructure with the thickness of 60 nm along in-plane (a) [100] direction and (b) [01-1] direction at the four electric field states.

Figs. S2(a) and (b) show the *M-H* curves of the γ'-Fe_4N film deposited on PMN-PT(011) substrate with the thickness of 60 nm along [100] and [01-1] directions at the four states. The SSE in the 60-nm-thick γ'-Fe_4N film can be ignore because of its large thickness, but the strain from the PMN-PT(011) substrate can also work. One can see there is almost no change of the *M-H* curves along [100] direction because of the relatively small strain [please see Fig. 4(b)]. However, when it comes to the [01-1] direction, the magnetization process becomes harder under the electric field of +10 kV/cm, which is contrary to the case of the 17-nm-thick sample [please see Fig. 2(b)]. So one can conclude that the strain effect plays an opposite role compared to the SSE, but the MEC influenced by strain effect is far less than SSE. Moreover, we know that the magnetostriction coefficient of γ'-Fe_4N is negative. So under the tensile strain along [01-1] direction, the magnetization process is supposed to become harder, which is corresponding to Fig. S2 (b).

3. Electric field tunable profiles of the FMR curves

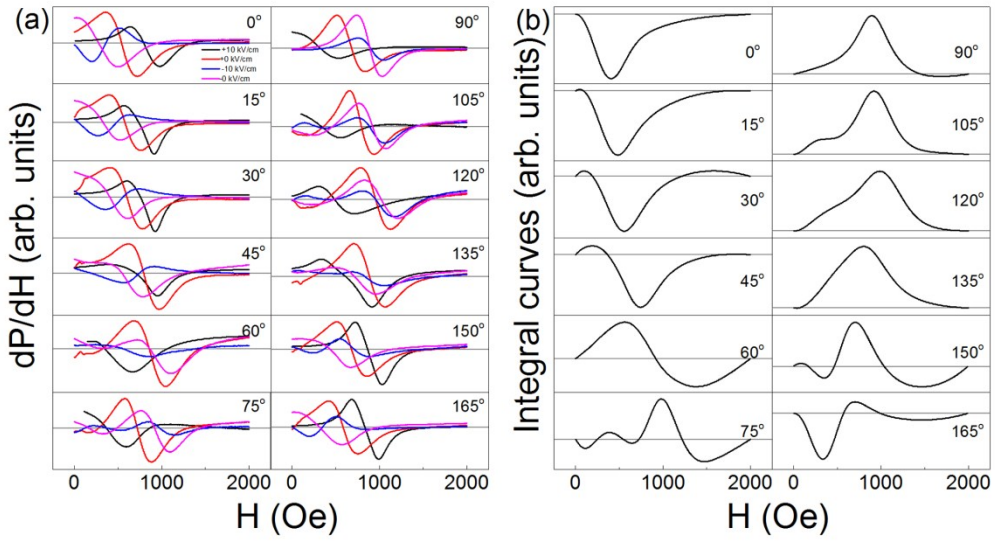

FIG. S3. (a) FMR derivative curves at the four states. (b) FMR integral curves at the -10 kV/cm state. The angels between the DC magnetic field and [100] direction of the sample are labeled in the figures.

From Fig. S3(a) one can see that the profile of the FMR curves at the -10 kV/cm state changes gradually from a reversed dispersive profile to a normal dispersive profile as the angle rotates from 0^o to 90^o. However, the other three states maintain the normal dispersive profile in spite of the change of the angle. Fig. S3(b) shows the FMR integral curves of the -10 kV/cm state in Fig. S3(a), which represents the FMR power absorption in the measurement. So one can see more clearly from Fig. S3(b) that there is completely negative power absorption at the state -10 kV/cm when the angle is 0^o, which indicates the negative damping. As the angle changes, the positive power absorption emerges. When the angle turns to 90^o, the power absorption is completely positive.

4. The total and partial densities of states (DOS) for γ'-Fe_4N

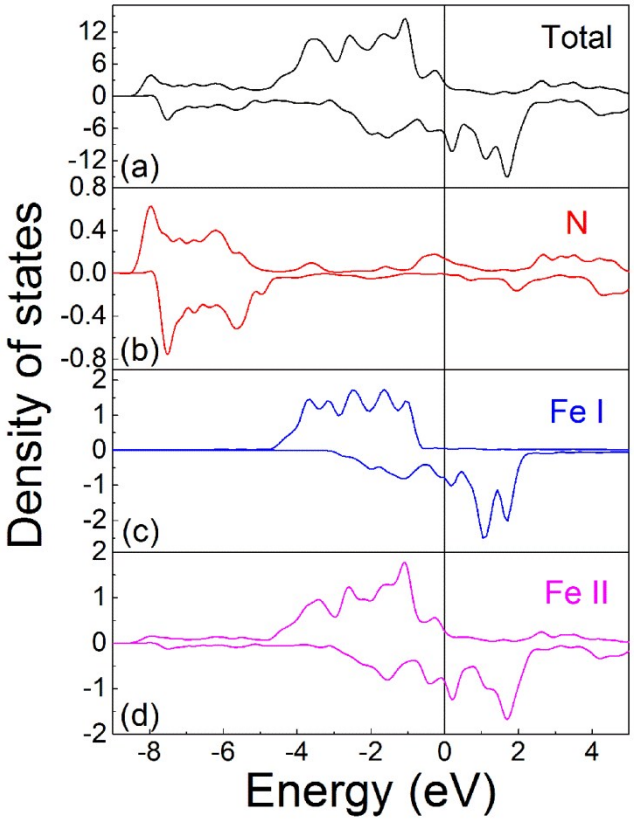

FIG. S4. The total and partial DOS for the [011] oriented γ'-Fe_4N in Fig. 6.

Fig. S4 shows the total and partial DOS of the γ'-Fe_4N lattice that we established in Fig. 6. All the images of DOS in Fig. S4 are the same as the previous results,[1,2] which confirms the accuracy of the simulations in this work.

5. The DOS of γ'-Fe_4N along [100] and [01-1] directions

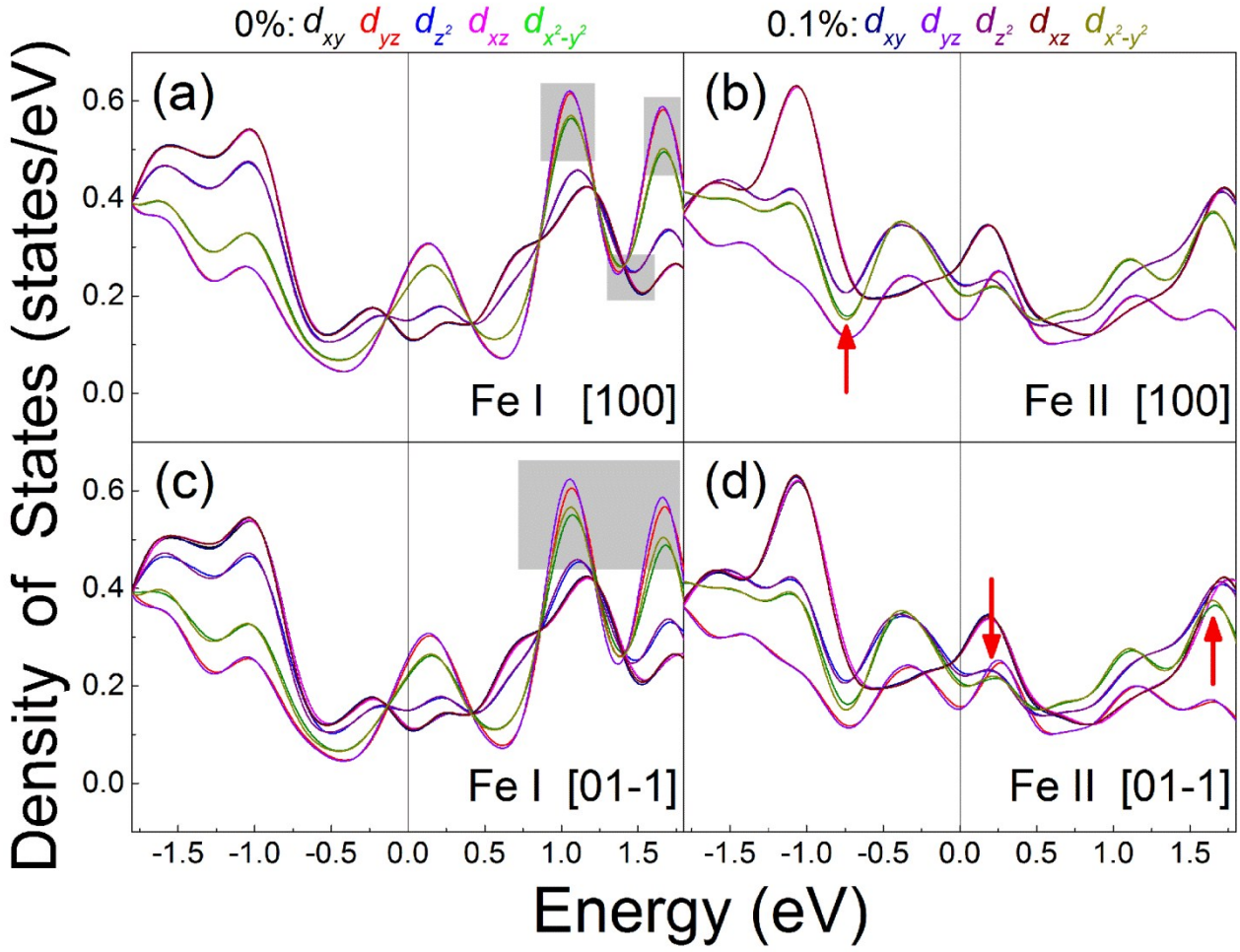

FIG. S5. Orbital-resolved density of states of the Fe atoms in relaxed γ'-Fe_4N and that subjected to the strain under the electric field of +10 kV/cm (~0.1%).

Fig. S5 shows the orbital-resolved DOS of Fe atoms in γ'-Fe_4N along [100] and [01-1] directions. One can see the difference under the two states of the strain is obvious (please see the areas marked by shadows and arrows). Moreover, for both Fe I and Fe II, the change of the DOS along [01-1] direction is larger than that along [100] direction, which is consistent with the experimental results in Figs. S2(a) and (b).

6. The DOS for the Fe atoms in the γ'-Fe_4N lattice near the interface of the sample under the four different electric field states simulated and calculated by first-principle calculation

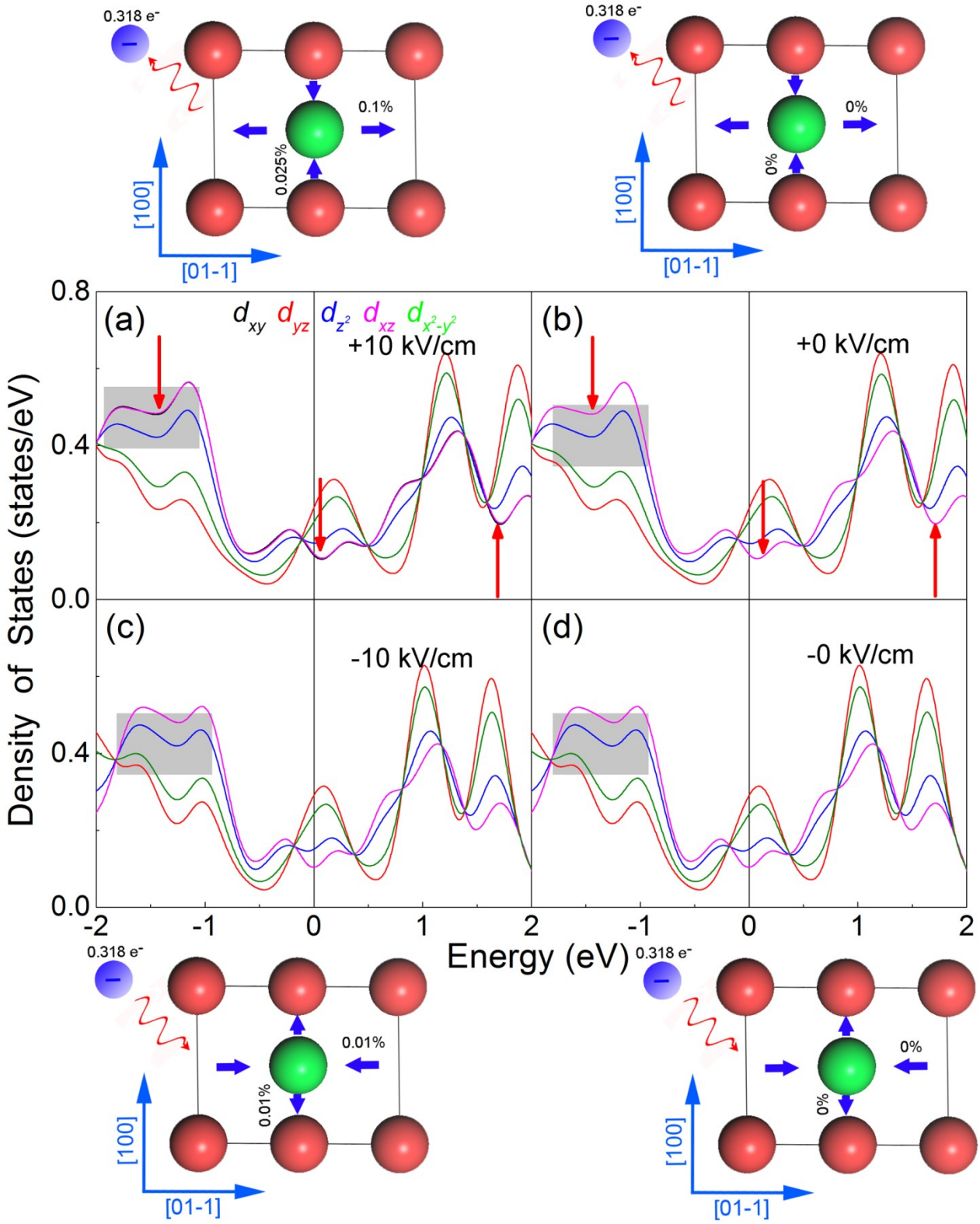

FIG. S6. Orbital-resolved DOS for the Fe I atom in γ'-Fe_4N under different electric field states along [100] direction.

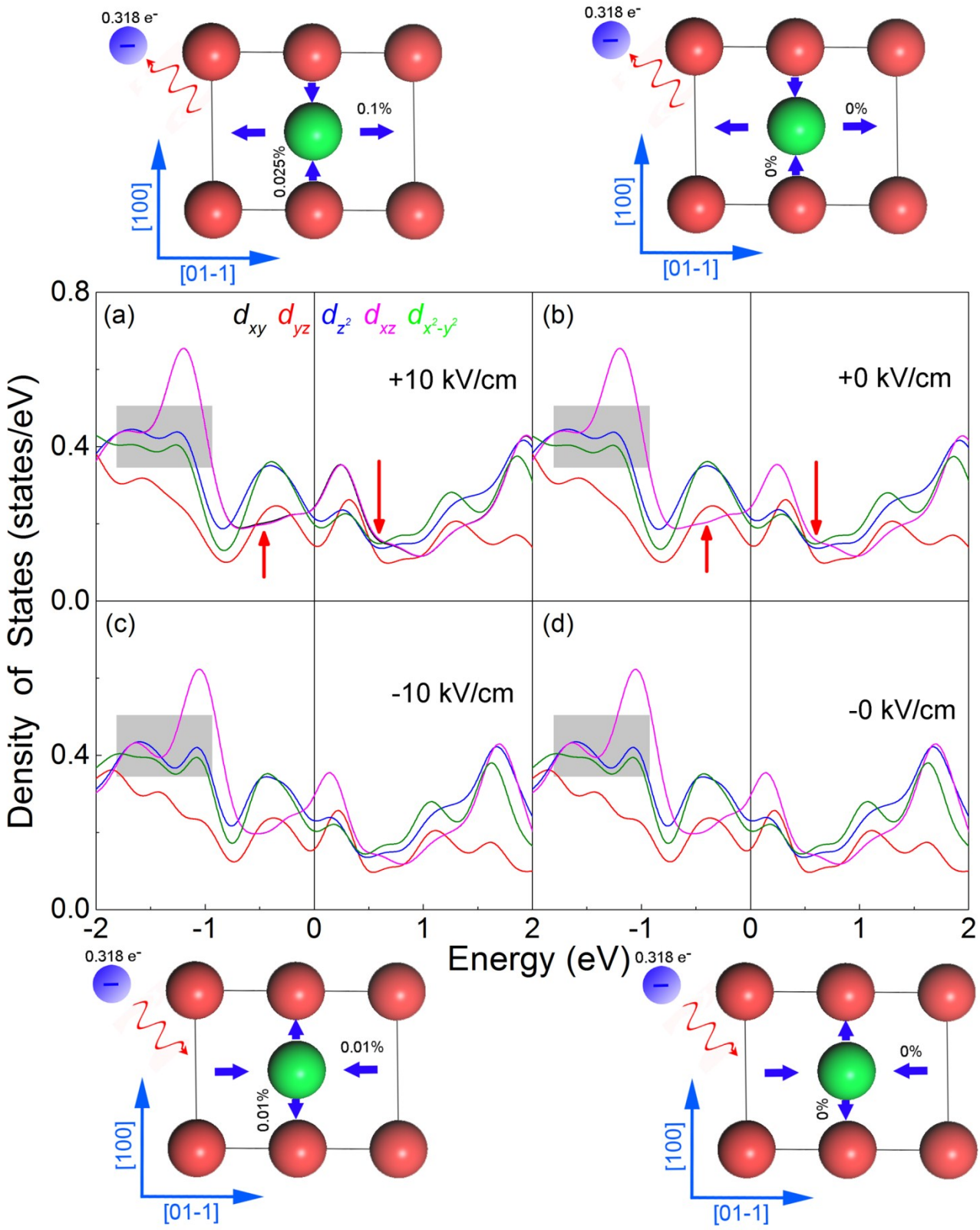

FIG. S7. Orbital-resolved DOS for the Fe II atom in γ'-Fe_4N under different electric field states along [100] direction.

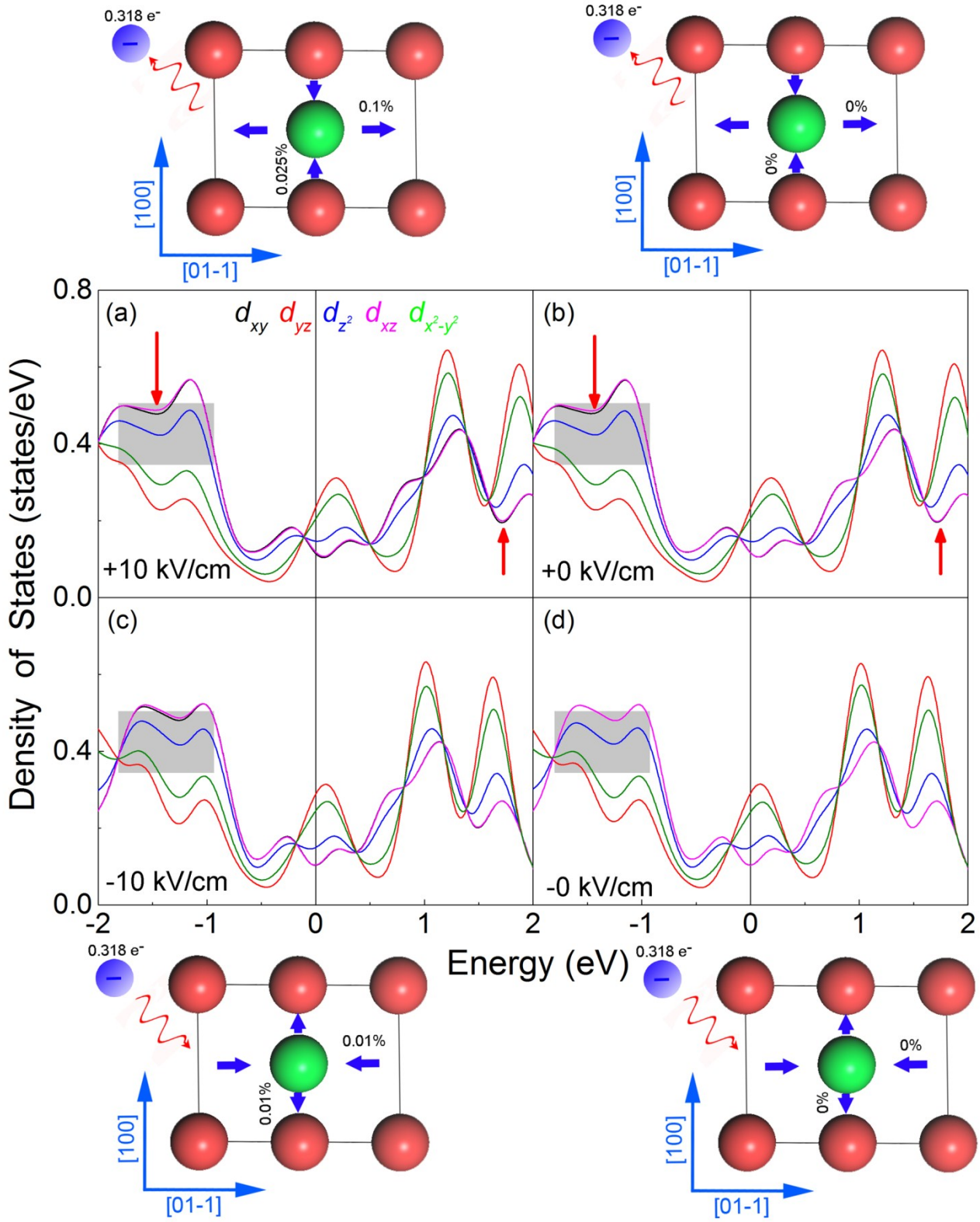

FIG. S8. Orbital-resolved DOS for the Fe I atom in γ'-Fe_4N under different electric field states along [01-1] direction.

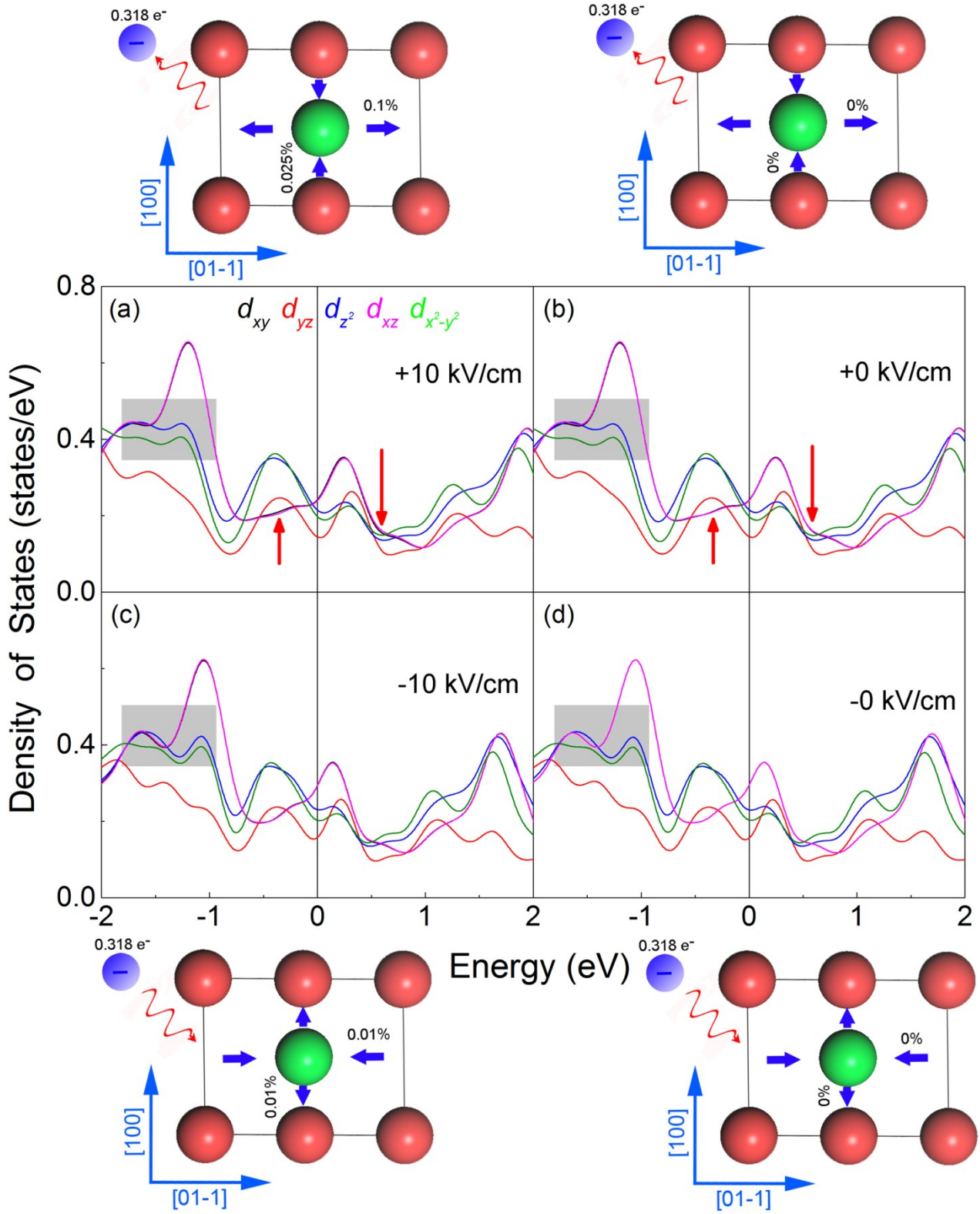

FIG. S9. Orbital-resolved DOS for the Fe II atom in γ'-Fe_4N under different electric field states along [01-1] direction.

From Figs. S6-S9, it is clear that the DOS is influenced greatly by the gain and loss of charge (for example, the parts in the shadows in Figs. S6-S9). However, just as mentioned in the text, the

electrostatic screening effect is confined by the surface screening length less than 1 nm for typical FM metals, so it can be ignored in this work, which can be confirmed by the experimental results in the text.[3-5] Moreover, the strain can also induce the difference of DOS between the states +10 kV/cm and +0 kV/cm (for example, the parts marked by red arrows in Fig. S6-S9). In addition, one can also see that the DOS between the states -10 kV/cm and -0 kV/cm are almost the same. It indicates that the tiny strain under the electric field of -10 kV/cm can hardly change the magnetism of γ'-Fe_4N, which is corresponding to the experimental results. It needs to be pointed out that the magnitudes of the strain at the states +10 kV/cm and -10 kV/cm used in the first-principle calculation are taken from the experimental values in Fig. 4(b). The gain and loss of the charge of the γ'-Fe_4N lattice at the interface is equal to the ferroelectric polarization P of the PMN-PT substrates, which can be acquired from the P-E curve in Fig. 4(a).

7. The magnetic domains measured by magnetic force microscope (MFM)

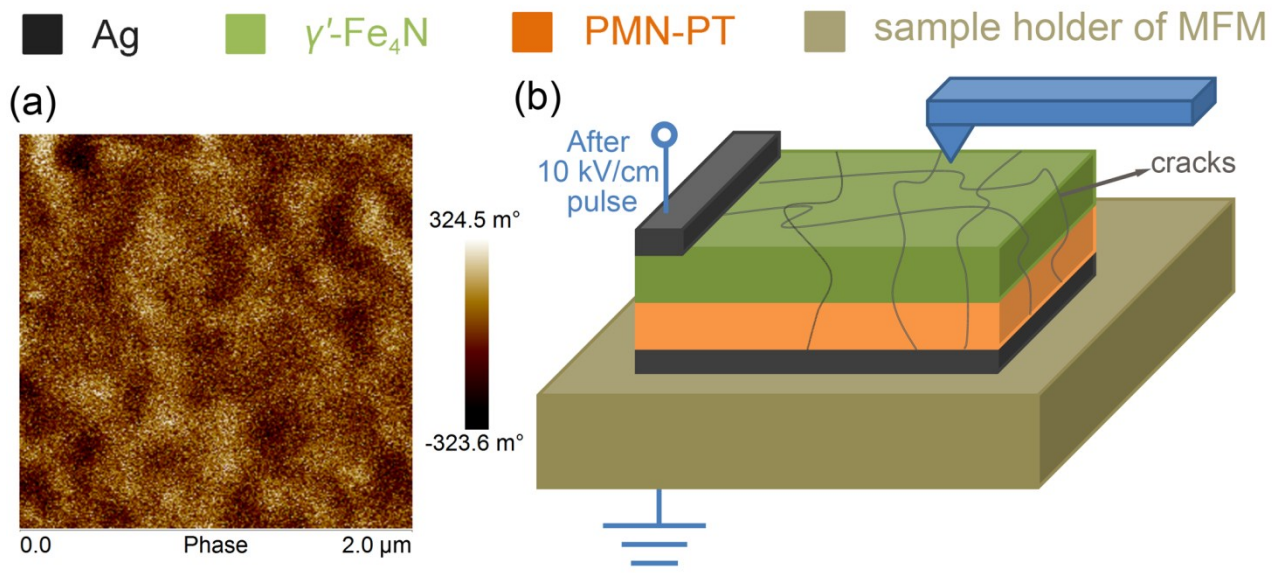

FIG. S10. (a) The MFM images of the γ'-Fe_4N/PMN-PT(011) heterostructure. (b) The schematic of the sample under a electric field during the measurement of MFM image.

Figs. S10(a) shows the MFM image of the γ'-Fe_4N/PMN-PT(011) heterostructure without electric field. We tried to investigate the alterations of the magnetic domains controlled by the electric fields. However, it could hardly be achieved by our MFM. During the measurement of the *M-H* curves and the ferromagnetic resonance, the electric field was applied through the electrodes (silver colloid) as is shown in Fig. 2(f) in the manuscript. However, during the measurement of MFM, the surface of the film needed to be exposed to the air and the sample was glued to the sample holder by silver colloid, where the schematic of the measurement is shown in Fig. S10(b). After the electric field pulse was applied to the sample through the holder of the MFM, we found that there were cracks on the sample [please see Fig. S10(b)]. The γ'-Fe_4N film became insulating because of these cracks, so the electric field couldn't be applied to the sample. The cracks were caused by the clamp force of the sample holder. We'll try to solve the problem in our future work.

The research of electric field control on the magnetic domains is attractive,[6,7] which definitely deserve to be investigated in the γ'-Fe_4N/PMN-PT(011) heterostructure.

REFERENCES

1 X. G. Ma, J. J. Jiang, P. Liang, J. Wang, Q. Ma and Q. K. Zhang, *J. Alloy. Compd.,* 2009, **480**, 475-480.

2 Z. R. Li, W. B. Mi and H. L. Bai, *Comp. Mater. Sci.,* 2018, **142**, 145-152.

3 T. X. Nan, Z. Y. Zhou, M. Liu , X Yang, Y. Gao, B. A. Assaf, H. Lin, S. Velu, X. J. Wang, H. S. Luo, J. Chen, S. Akhtar, E. Hu, R. Rajiv, K. Krishnan, S. Sreedhar, D. Heiman, B. M. Howe, G. J. Brown and N. X. Sun, *Sci. Rep.,* 2014, **4**, 3688.

4 C. L. Jia, T. L. Wei, C. J. Jiang, D. S. Xue, A. Sukhov and J. Berakdar, *Phys. Rev. B,* 2014, **90**, 054423.

5 M. Weisheit, S. Fähler, A. Marty, Y. Souche, C. Poinsignon and D. Givord, *Science,* 2007, **315**, 349-351.

6 H. E. L. Tuomas, J. A. F. Kvin and van D. Sebastiaan, *Sci. Rep.,* 2012, **2**, 258.

7 M. Buzzi, R. V. Chopdekar, J. L. Hockel, A. Bur, T. Wu, N. Pilet, P. Warnicke, G. P. Carman, L. J. Heyderman and F. Nolting, *Phys. Rev. Lett.,* 2013, 1**11**, 027204.